

Modeling the transport of cosmic ray due to long term variation using a stochastic differential method

Gang Li *, G. M. Webb *, J.A. le Roux *, M. Wiedenbeck †, V. Florinski * and G. P. Zank *

* Center of Space Plasma and Aeronomics, University of Alabama, Huntsville, AL 35899, USA

† Department of Physics, University of Alabama, Huntsville, AL 35899, USA

† Jet Propulsion Laboratory, California Institute of Technology, Pasadena, CA 91125, USA.

Abstract. The propagation of cosmic rays in the solar system is subject to both transients and long term variations in the solar wind. The effect of long term variation such as the solar cycle effect can be best seen from the hysteresis effect of galactic cosmic rays (GCRs). A recent study by Wiedenbeck *et al.* [1], for example, showed that the intensities of GCR Carbon and Oxygen at 226 MeV/nuc are consistently higher in the declining solar activity phase than in the rising phase when the corresponding intensities at 64 MeV/nuc are at comparable values. A proper understanding of this observation requires solving the time dependent transport equation. We discuss here the first attempt of solving a time dependent GCR modulation using a stochastic differential equation method. Such a technique have been used previously to obtain steady state solutions of the transport equation and has been shown to be equivalent to traditional finite difference method. The advantage of a stochastic differential equation approach is that it allows one to obtain the probability distribution function of travel time and the Green's function of the transport equation as a function of solar cycle. We restrict ourselves to a simple 1D model to illustrate the essence of the physics.

Keywords: Modulation, time-dependent transport, Stochastic differential equation

I. INTRODUCTION

Galactic cosmic rays (GCRs) reaching 1 AU at the Earth are modulated by magnetic field carried out in the radially expanding solar wind. The modulation effect is represented by one single modulation parameter ϕ in the so-called force field model [2], where the steady state solution of the cosmic ray transport equation [3],

$$\frac{\partial f}{\partial t} + V_{sw} \cdot \nabla f - \nabla \cdot (\kappa \cdot \nabla f) - \frac{1}{3} \nabla \cdot V_{sw} \frac{\partial f}{\partial \ln p} = 0 \quad (1)$$

is replaced by requiring the particle current $S = CV_{sw}U_p - \kappa \cdot (\nabla U_p)$ to be zero, where $C = -\frac{1}{3} \frac{\partial \ln f}{\partial \ln p}$ is the Compton-Getting factor and $U_p = 4\pi p^2 f$ is the differential number density. In equation (1), r and V_{sw} are the radial distance from the Sun and the solar wind speed; κ is the diffusion coefficient of GCR. The force-field approximation is based on the assumption that $V_{sw}r/\kappa \ll 1$ (diffusion dominate over advection) and

it works better for higher energy GCRs as κ 's for these particles are larger.

In a 1D spherical symmetric geometry, the simplification used in [2] leads to the replacement of the second order Fokker Planck equation (1) by a first order equation

$$\frac{pV_{sw}}{3\kappa_{rr}} \frac{\partial f}{\partial p} + \frac{\partial f}{\partial r} = 0 \quad (2)$$

where κ_{rr} is the radial diffusion coefficient and V_{sw} is the radial solar wind speed. This simplification leads to $f(p, r) = f(p^*, R)$ where R is the outer boundary and p^* is the particle momentum at R when tracing back along a characteristic line from (r, p) . The value of p^* is decided from [4],

$$\int_p^{p^*} \frac{\kappa_2 \beta}{p'} dp' = \int_r^R \frac{V_{sw}}{3\kappa_1} dr = \phi(r) \quad (3)$$

where $\kappa_{rr} = \beta \kappa_1(r) \kappa_2(P)$ is assumed and $\beta = v/c$ is the particle speed divided by the speed of light and $P = pc/qe$ is the particle rigidity. The unit of κ_2 is GV . One can show that in the "force-filed" approximation the kinetic energy loss of a charged particle with charge Z from R to r is $Ze\phi$ [4]. Note, this energy loss in the force-field model is not the same as the adiabatic energy loss from the transport equation (1).

The force-field model ignores the presence of the solar wind Termination Shock (TS) and thus does not account for any possible energy increases due to particle acceleration in the heliosheath and at the TS. The effects of particle energy increase due to acceleration at the TS has been discussed by Jokipii *et al.* and Caballero-Lopez *et al.* [5], [6].

The hysteresis effect has been considered in a 1D geometry first by O' Gallagher [7]. Later Chi & Lee [8] studied the hysteresis effect using a response function method and assumed κ varies sinusoidally with time. Similar calculations has been carried out by Steenkamp & Moraal [9], who employed the traditional finite difference method. They also argued that the effects of including latitudinal transport due to a two-dimensional geometry can reduce the hysteresis effects significantly. More sophisticated models, in particular those include drift effects have also been constructed (e.g. [10], [11]). These early studies revealed that a proper understanding

of the hysteresis phenomenon requires a thorough understanding of how cosmic rays respond to various time-varying conditions in the heliosphere. These time variations include a wavy Heliospheric Current Sheet (HCS); time-dependent gradient, curvature and current-sheet drifts and transient outpropagating diffusion barriers, such as Global Merged Interaction Regions (GMIRs). These works have shown that while the effects of the drift could dominate the modulation during solar minimum, the more wavy current sheet, Coronal Mass Ejections (CMEs) and GMIRs play more important roles during solar maximum. Clearly, to include the effect of the drift velocity and a wavy HCS, one needs to consider a 2-D or 3-D simulation. However, such a simulation will blend in many complex physical inputs and the interpretation of the simulation results can be rather complicated. In contrast, the fact that the observations in [1] can often be reasonably explained by a simple 1D force-field model prompts us to consider a 1D time-dependent model of GCR modulation in this work. We therefore note that the model considered here should be viewed more qualitatively rather than quantitatively. Extension to a 2D/3D model will be pursued in the future.

We employ a stochastic differential equation method to solve the transport equation. The stochastic differential equation method is used to solve Fokker-Planck type differential equations owing to its simple mathematical formalism, ease of programming as well as the supercomputational power of today's modern computers. It has been adopted in studying the transport of cosmic rays [12], [13]. In particular, *Ball et al.* [13] discussed the modulation of GCR using the stochastic differential equation method in a 3D geometry. Our procedure is similar to that used in [13] but differs in that we include explicitly the time-dependent solar cycle effect due to a time-varying κ , while that of [12], [13] only treated steady-state solution.

Our model represents the first attempt of solving the time-dependent transport equation using a stochastic differential method. It is based on the backward Kolmogorov equation. *Yamada et al.* [14] discussed a forward Kolmogorov equation approach in modeling the hysteresis effect. However, [14] ignored an effective loss term in their equation (2), leading to an exaggerated effect. Our approach can be also understood from the Feynman-Kac formula and its physical meaning is related to the Green's function method, which we discuss in our paper.

II. MODEL DESCRIPTION

Two time scales are essential in understanding the time-dependent modulation and the hysteresis effects. The first is the solar cycle period $T = 11$ years; the second is the travel time τ of a GCR from the solar wind boundary to 1 AU. A rough estimate of τ is $\tau \sim R^2/(3\kappa_{rr})$; taking $R = 90$ AU and an r -independent $\kappa_{rr} = 6 * 10^{22} \beta(P/1\text{GV})\text{cm}^2/\text{s}$ [6], we

find $\tau \sim 0.82$ years for O^{8+} with a kinetic energy of $E_k \sim 76$ MeV/nuc. If κ_{rr} is 3.5 times smaller at solar maximum, $\tau \sim 2.87$ years. Since a cosmic ray loses energy as it propagates into the solar system, τ shall be somewhat larger. When τ is comparable to $\sim T/2$, a time-dependent solution of the transport equation is needed to construe the hysteresis effects.

The transport equation in 1D spherically symmetric geometry is,

$$\frac{\partial f}{\partial t} = \kappa_{rr} \frac{\partial^2 f}{\partial r^2} + \left[\frac{\partial(r^2 \kappa_{rr})}{r^2 \partial r} - V_{sw} \right] \frac{\partial f}{\partial r} + \frac{\partial(r^2 V_{sw})}{3r^2 \partial r} \frac{\partial f}{\partial \ln p}. \quad (4)$$

Equation (4) is written in a form that can be readily translated to a set of equations that describe the motion of a quasi particle, which are (see e.g. [15]),

$$ds = -dt \quad (5)$$

$$dp/p = 2/3(V_{sw}/r)ds \quad (6)$$

$$dr = \left(\frac{2\kappa_{rr}}{r} + \frac{\partial \kappa_{rr}}{\partial r} - V_{sw} \right) ds + \text{erf}^{-1}(\xi) \sqrt{4\kappa_{rr}} ds \quad (7)$$

Here $dt < 0$ as it is a backward stochastic process; $\text{erf}(x)$ is the error function and ξ is an evenly distributed random number between (0, 1).

Note $\text{erf}^{-1}(\xi)$ is a Gaussian random number, so $\text{erf}^{-1}(\xi)/\sqrt{2ds}$ is a Wiener process. In obtaining equation (6), we have assumed V_{sw} to be radial independent. Note that in evaluating dr , $(\frac{1}{r^2} \frac{\partial(r^2 \kappa_{rr})}{\partial r} - V_{sw})$ depends on the r -dependence of κ_{rr} . Theoretical work [16] suggested that κ_{rr} is a constant in the outer heliosphere and increase linearly with r in the inner heliosphere. Observationally, *Cummings & Stone* [17] found that the r -dependence of κ_{rr} near solar maximum is weak in the outer heliosphere (see however, [18] where a $r^{1.4}$ and $r^{1.1}$ dependences of λ_r in the outerheliosphere for Cycles 20/22 ($A > 0$) and Cycle 21 ($A < 0$) are found). In this work, for simplicity we follow [1] and assume an r -independent κ_{rr} . To obtain $f(p)$, an ensemble of paths described by equations (5), (6) and (7) that start at 1 AU with momentum p and ends at R with momentum p' (backward in time) are followed and all paths are averaged with a weight of $f_b(p')$ for each path.

By following single (quasi) particle motion in the solar wind, our approach takes a microscopic point of view of the problem and differs from a traditional finite difference method where the distribution function f is solved directly. Conceptually, this approach can be understood from the Green's function method [19] in which solving the transport equation (1) is achieved by obtaining $f(r, p, t)$ from the convolution of the Green's function $G(R, p', t'; r, p, t)$ with the GCR spectrum at the boundary according to [4],

$$\begin{aligned} f(r, p, t) &= \int \int G(R, p', t'; r, p, t) f_b(p') dp' dt' \\ &= \int \tilde{G}(R, p'; r, p, t) f_b(p', t') dp'. \end{aligned} \quad (8)$$

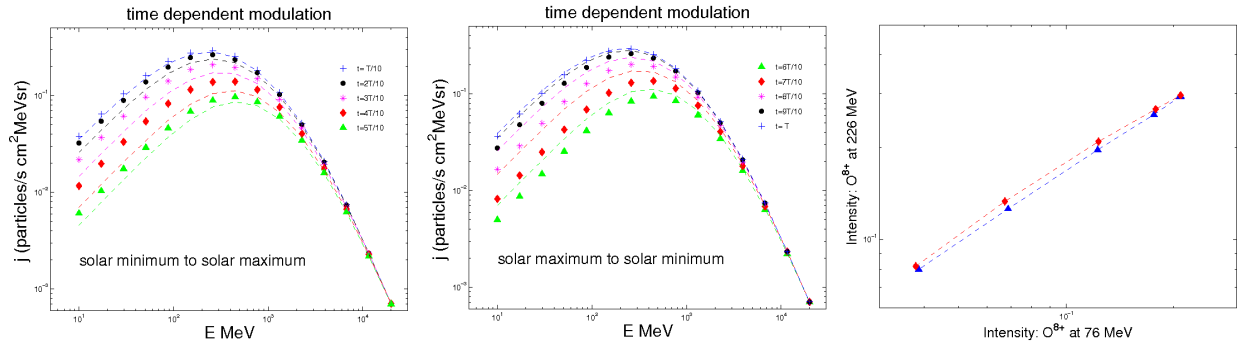


Fig. 1. Time dependent modulation. The left two panels are for the period from Solar Minimum (Solar Maximum) to Solar Maximum (Solar Minimum). The right panel shows the correlation between $E = 76$ MeV/nucleon oxygen and $E = 226$ MeV/nucleon oxygen. These two energies correspond to the lowest and highest energy measured by CRIS on-board of ACE. See text for details.

where $G(R, p', t'; r, p, t)$ is the solution of

$$\frac{\partial G}{\partial t} + V_{sw} \cdot \nabla G - \nabla \cdot (\kappa \cdot \nabla G) - \frac{1}{3} \nabla \cdot V_{sw} \frac{\partial G}{\partial \ln p} = \delta(r - r') \delta(p - p') \delta(t - t'). \quad (9)$$

In obtaining the last line of equation (8), we assume the boundary $f_b(p')$ is time independent, so that the $\int dt'$ integral of $\int G(R, p', t'; r, p, t)$ becomes $\tilde{G}(R, p'; r, p, t)$. If one is to study the effect of the Sun being in different regions in the local interstellar medium, one can throw in a time dependent $f_b(p', t')$, which varies much slower comparing to the 11 years solar cycle. Clearly $G(R, p', t'; r, p, t)$ describes the transition probability from an initial state (R, p', t') to a final state (r, p, t) . In this formalism, the ensemble average of each individual path in the Monte-Carlo simulation gives the solution of $\tilde{G}(R, p'; r, p, t)$.

We now discuss our model assumptions. We assume a κ_{rr} given by (similar to [8]),

$$\kappa_{rr}(r) = \frac{\kappa_B + \kappa_S}{2} + \frac{\kappa_B - \kappa_S}{2} * \cos\left(2\pi \frac{t - r/V_{sw}}{T}\right) \quad (10)$$

where κ_B and κ_S are the diffusion coefficients at solar minimum and solar maximum and $T = 11$ years is the solar activity period. We take $\kappa_S = 6 \times 10^{22} \text{ cm}^2/\text{s}$ and $\kappa_B = 3.5\kappa_S$. We assume the turbulence is carried out by the solar wind with a speed of $V_{sw} = 400$ km/s, hence the term $(t - r/V_{sw})$ in equation (10). More complicated time dependence, that mimic high speed streams and CIRs in the solar minimum can be considered. These structures can slow down the propagation of GCRs from outer heliosphere into the inner heliosphere, leading to an intermittent κ_{rr} . For the outer boundary, we assume a boundary at $R = 90$ AU and ignore GCR modulation in the heliosheath and the effects of the termination shock (TS). We further assume a simple power law of $j(E) \sim E^{-2.35}$ for the source spectrum at the outer boundary where E is the total energy of an GCR particle and j is the current flux. A more sophisticated shape of f_b taking into account of interstellar physics has been discussed in [20].

III. RESULTS AND DISCUSSION

We first study the time dependence of GCR modulation. The left two panels of figure 1 plot the modulated spectrum at 1 AU at 10 different times, $t_1 = T/10$, $t_2 = 2T/10$, ..., and $t_{10} = T$ with the reference time at $t = 0$ taken to be at solar minimum (solar maximum). In the first panel, from top to bottom, the symbols “+”, “•”, “*”, filled “◊” and filled “△” are the solutions of the time dependent transport equation from t_1 to t_5 . The dashed curves of the same color are the steady state solution with κ evaluated at the corresponding time and at the Sun (i.e. $r = 0$). In the second panel, from bottom to top, the symbols of filled “△”, filled “◊”, “+”, “•” and “*” are the solutions of the time dependent transport equation from t_6 to t_{10} , while the dashed curves of the same color are the steady state solution with κ evaluated at the corresponding time and at the Sun. The difference between the steady state solutions and the time dependent solutions is clearly seen. During the declining phase in the first panel, the time dependent solutions are systematically larger than the steady state solutions. This trend reverse during the recovering phase, as seen in the second panel.

On the rightmost panel of figure 1, we plot the correlation of the O^{8+} intensities for 76 MeV/n and 226 MeV/n for one solar cycle. The blue dashed curve with filled “△” is for the period of solar minimum to solar maximum and the red dashed curve with “◊” is for the period of solar maximum to solar minimum. Clearly, for the same intensity of oxygen at 76 MeV/nucleon near solar maximum, the intensity of oxygen at 226 MeV/nucleon in the recovering phase (red curve) is higher than that in the depleting phase (blue curve). Indeed, the intensity of O^{8+} at 226 MeV/nuc at t_7 is about 6% larger than that at t_4 , while the intensity of oxygen at 76 MeV/nuc at these two times are almost equal. This 6% increase is to be compared with the observed $\sim 10\%$ increase [1].

We next plot the distribution of the travel time of cosmic rays for the two energies considered. Figure 2 plots the probability density of finding a cosmic ray oxygen arriving at 1 AU with a kinetic energy of 76 MeV

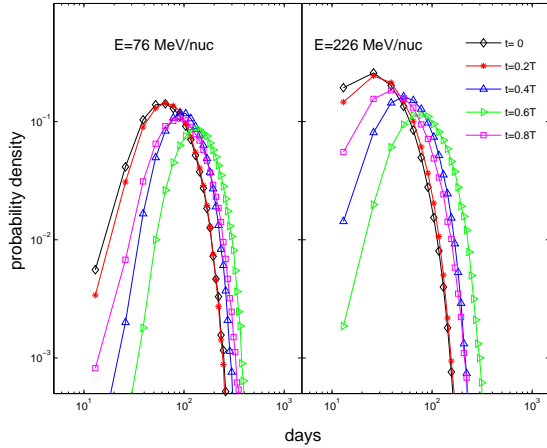


Fig. 2. The probability distribution of the travel time for $E = 76$ MeV/nucleon oxygen (left panel) and $E = 226$ MeV/nucleon oxygen (right panel).

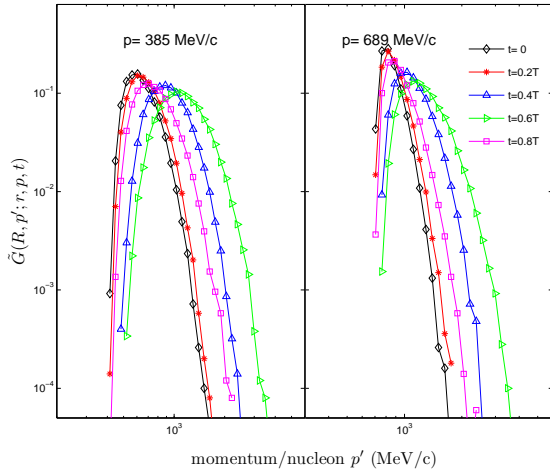


Fig. 3. Plot of the Green's function $\tilde{G}(R, p'; r, p, t)$ for 5 different times. Left panel for $p = 385$ MeV/c and right panel for $p = 689$ MeV/c. See text for details.

(left panel) and 226 MeV (right panel) as a function of solar cycle with $t = 0$ corresponding to a solar minimum. Define the most probable travel time t_p as the time having the maximum probability in figure 2, we find that t_p becomes ~ 60 days for a 76 MeV/nucleon oxygen near solar minimum (the black and the red curves). This time becomes larger when t approaches a solar maximum, becoming ~ 180 days at $t = 0.6T$, about 3 times larger than near the solar minimum. It then decreases as it approaches the next solar minimum, becoming 100 days at $t = 0.8T$. Similar behavior is also found for 226 MeV/nucleon oxygen, where the most probable time t_p is about 25 days near solar minimum, and increases to ~ 100 days at $t = 0.6T$ (near solar maximum) before dropping to ~ 60 days at $t = 0.8T$.

Finally, we plot the Green's function $\tilde{G}(R, p'; r, p, t)$ in figure 3. The two kinetic energies considered, $E = 76$

MeV/nucleon and $E = 226$ MeV/nucleon, translate to $p = 385$ MeV/c and $p = 689$ MeV/c respectively. The left panel shows $\tilde{G}(R, p'; r, p, t)$ for $p = 385$ MeV/c and the right panel shows $\tilde{G}(R, p'; r, p, t)$ for $p = 689$ MeV/c. From the figure we find that the peaks of the Green's function have slight higher initial p 's than the arrival p 's. This is due to particle energy loss during its propagation. Also note the initial p' shifts to the right as time goes from solar minimum to solar maximum. This reflects the fact that the longer a cosmic ray stays in the solar system, the more energy it loses.

In summary, we present in this paper a 1D time-dependent modulation calculation to investigate the solar activity cycle effects on GCR modulation. Our simulation is based on the stochastic differential equation method. In our model, the effects from the drift and a wavy HCS are ignored and the solar cycle variance is modeled by a time-dependent κ_{rr} . Our simulation results show that $\sim 50\%$ of the observed hysteresis effect can be ascribed to a periodical change of κ_{rr} with its maximum at solar minimum 3.5 times larger than its minimum at solar maximum. It provides a basis to explain the observations of [1]. Using a stochastic differential equation method, we also obtain the distribution of cosmic ray travel time and the Green's function as a function of solar cycle, which are shown in figure 2 and figure 3.

IV. ACKNOWLEDGMENTS

This work has been supported in part by NASA grants NNX06AC21G, NNX07AL52A. GL acknowledges useful discussions with Dr. Yan Wang.

REFERENCES

- [1] Wiedenbeck, M. E., et al., 29th ICRC Proceedings, 277, 2005.
- [2] Gleeson, L. J. & Axford, I., 1968, *Astro. Phys. J.*, 154, 1011.
- [3] Parker, E. N., 1965, *Planet. Space. Sci.*, 13, 9.
- [4] Gleeson, L. J. & Webb, G., 1980, *Fundamentals of Cosmic Physics*, 6, 187.
- [5] Jokipii, J.R., J. Kóta and E. Merenyi, 1994, *Astro. Phys. J.*, 111, 345.
- [6] Caballero-López, R. A.; Moraal, H.; McDonald, F. B., 2006, *Geophys. Res. Lett.*, 33.
- [7] O'Gallagher, 1975, *Astro. Phys. J.*, 197, 495.
- [8] Chih, P. P.; Lee, M. A., 1986, *J. Geophys. Res.*, 91, 2903-2913.
- [9] Steenkamp, R and Moraal, H., 1993, 23th ICRC Proceedings, 3, 539-542.
- [10] Kota, J.; Jokipii, J. R., 1983, *Astro. Phys. J.*, 265, p573.
- [11] le Roux, J. A.; Potgieter, M. S., 1990, *Astro. Phys. J.*, 361, 275.
- [12] Zhang, M. 1999, *Astro. Phys. J.*, 513, 409.
- [13] Ball, B., Zhang, M., Rassoul, H. and Linde, T., 2005, *Astro. Phys. J.*, 634, 1116.
- [14] Yamada, Y., Yanagita, S., Yoshida, T., 1999, *Adv. Space Res.*, 23, 505.
- [15] Schuss, Zeev, 1980, *Theory and Applications of Stochastic Differential Equations*, New York, John Wiley, 1980.
- [16] Zank, G. P.; Matthaeus, W. H.; Smith, C. W., 1996, *J. Geophys. Res.*, 101, 17093.
- [17] Cummings, A. C.; Stone, E. C., 2003, 28th ICRC Proceedings, 3897.
- [18] Fujii, Z., McDonald, F. B., 2005, *Adv. Space Res.*, 35, 611.
- [19] Webb, G. M., 1981, *Astrophys. Space. Sci.*, 80, 323.
- [20] Webber, W. R. and Lockwood, J. A., 2001, *J. Geophys. Res.*, 106, 29323.